

## Surface Plasmon Polariton-Induced Hot Carrier Generation for Photocatalysis

Wonmi Ahn,<sup>1</sup> Daniel C. Ratchford,<sup>2</sup> Pehr E. Pehrsson,<sup>2</sup> and Blake S. Simpkins<sup>2,\*</sup>

<sup>1</sup>National Research Council Postdoctoral Associate, U.S. Naval Research Laboratory, Washington, DC 20375, United States

<sup>2</sup>Chemistry Division, U.S. Naval Research Laboratory, Washington, DC 20375, United States

\*E-mail: [blake.simpkins@nrl.navy.mil](mailto:blake.simpkins@nrl.navy.mil)

### Supporting Information

#### Contents

Photon-to-Hot Carrier Conversion Efficiency Calculation.

Estimation of a Temperature Increase through Plasmonic Heating.

Tunneling Probability.

Supporting Figures.

**Figure S1.** SPP dispersion curves.

**Figure S2.** Data processing for photovoltage and photocurrent responses.

**Figure S3.** Anodic half-reaction of photocatalytic water-splitting.

**Figure S4.** Characterization of ALD grown TiO<sub>2</sub> films.

**Figure S5.** Photoluminescence from a TiO<sub>2</sub> layer.

**Figure S6.** Open-circuit voltage of a bare TiO<sub>2</sub> film.

**Figure S7.** Open-circuit voltage versus time profiles of (a) Au/TiO<sub>2</sub> and (b) Au only system.

**Photon-to-Hot Carrier Conversion Efficiency Calculation.** We calculated the photon-to-carrier conversion efficiency,  $\eta$ , by taking the ratio of photocurrents measured by our working electrodes (electrons per second) to the number of photons incident on the half-ball lens per second. Photocurrents measured in Ampere (Coulombs per second) from the electrochemical cell were first converted to electrons per second by converting Coulombs to electron charge as  $1 e = 1.602 \times 10^{-19} C$ . The illumination laser power measured by a power meter in Watts was converted to photons per second by dividing the power (Joules per second) by photon energy ( $E$ , Joules per photon). The photon-to-hot carrier conversion efficiency was then calculated according to Eq. S1 and listed in **Table S1** for different metal films and lasers.

$$\eta = \frac{\text{Photocurrent (electrons/sec)}}{\text{Illumination Intensity (photons/sec)}} \times 100 \quad (\text{Eq. S1})$$

**Table S1.** Photon-to-hot carrier conversion efficiency.

Working electrodes	Laser (nm)	Laser power (W)	Current (A)	Efficiency (%)
Ag/TiO <sub>2</sub>	785	3.2x10 <sup>-3</sup>	1.4x10 <sup>-11</sup>	7.0x10 <sup>-7</sup>
		3.3x10 <sup>-2</sup>	2.6x10 <sup>-11</sup>	1.2x10 <sup>-7</sup>
	532	2.1x10 <sup>-6</sup>	4.0x10 <sup>-11</sup>	4.7x10 <sup>-3</sup>
		1.3x10 <sup>-5</sup>	6.2x10 <sup>-10</sup>	1.1x10 <sup>-2</sup>
		2.3x10 <sup>-5</sup>	8.4x10 <sup>-10</sup>	8.4x10 <sup>-3</sup>
Au/TiO <sub>2</sub>	785	1.4x10 <sup>-2</sup>	2.5x10 <sup>-11</sup>	2.9x10 <sup>-7</sup>
		1.3x10 <sup>-2</sup>	2.5x10 <sup>-11</sup>	3.1x10 <sup>-7</sup>

**Estimation of a Temperature Increase through Plasmonic Heating.** Although the linear dependence of photocurrent on illumination power is a clear indication of a photocarrier-driven process, we further substantiate this assignment by calculating the maximum temperature increase the system could possibly experience. Heating of the face of a metal slab by laser irradiation follows<sup>1</sup>

$$\Delta T = \frac{H}{k} \sqrt{\frac{4\alpha t}{\pi}} \quad (\text{Eq. S2})$$

where  $\Delta T$  is the temperature rise,  $H$  is the absorbed laser energy,  $k$  is the thermal conductivity of gold ( $310 \text{ W/m} \cdot \text{K}$ ),  $\alpha$  is the thermal diffusivity ( $3.2 \times 10^{-5} \text{ m}^2/\text{s}$  for a 50 nm thin film)<sup>2</sup> and  $t$  is time. Making the most generous assumptions to maximize temperature rise (e.g., inserting the highest laser power used in this study, 33 mW, and assuming that *all* laser energy is absorbed in the film and that energy does not dissipate from the slab), results in a calculated rise of  $<1 \text{ }^\circ\text{C}$  for the illumination times used. Simply reducing the inserted laser power to that used for the majority of experiments reduces this predicted temperature increase by an order of magnitude and properly considering only partial photon absorption as well as heat dissipation into solution would decrease this temperature rise even further. These calculations confirm that heating is not responsible for the electrochemical responses presented in this work.

**Tunneling Probability.** Estimates of tunneling probability can be calculated according to the following expression.<sup>3</sup>

$$T_t = \frac{16E(E_0 - E)}{E_0^2} \exp\left(-2W \sqrt{\frac{2m^*(E_0 - E)}{\hbar^2}}\right) \quad (\text{Eq. S3})$$

$T_t$  is the tunneling probability,  $E$  the energy of the carrier,  $E_0$  the barrier height,  $W$  the barrier width,  $m^*$  the effective mass of the tunneling carrier ( $0.8 \cdot m_e$  for holes in  $\text{TiO}_2$ )<sup>4</sup> and  $\hbar$  is Planck's constant. If one assumes the only state available to accept a tunneling hole from the metal is located 0.4 eV below the Fermi level (this is the redox potential of the OH oxidation reaction), the tunneling probability is  $\sim 10^{-59}$  due primarily to the large ( $\sim 2.2$  eV) and somewhat thick (10 nm) barrier. Even if one assumes the carriers may tunnel into a continuum of states spanning the entire region below the Fermi level and considering the most highly excited holes possible ( $\sim 0.3$  from the  $\text{TiO}_2$  valence band), tunneling probability is still only  $\sim 10^{-22}$ . Therefore, even for the most energetic carriers created in this study, tunneling is negligible.

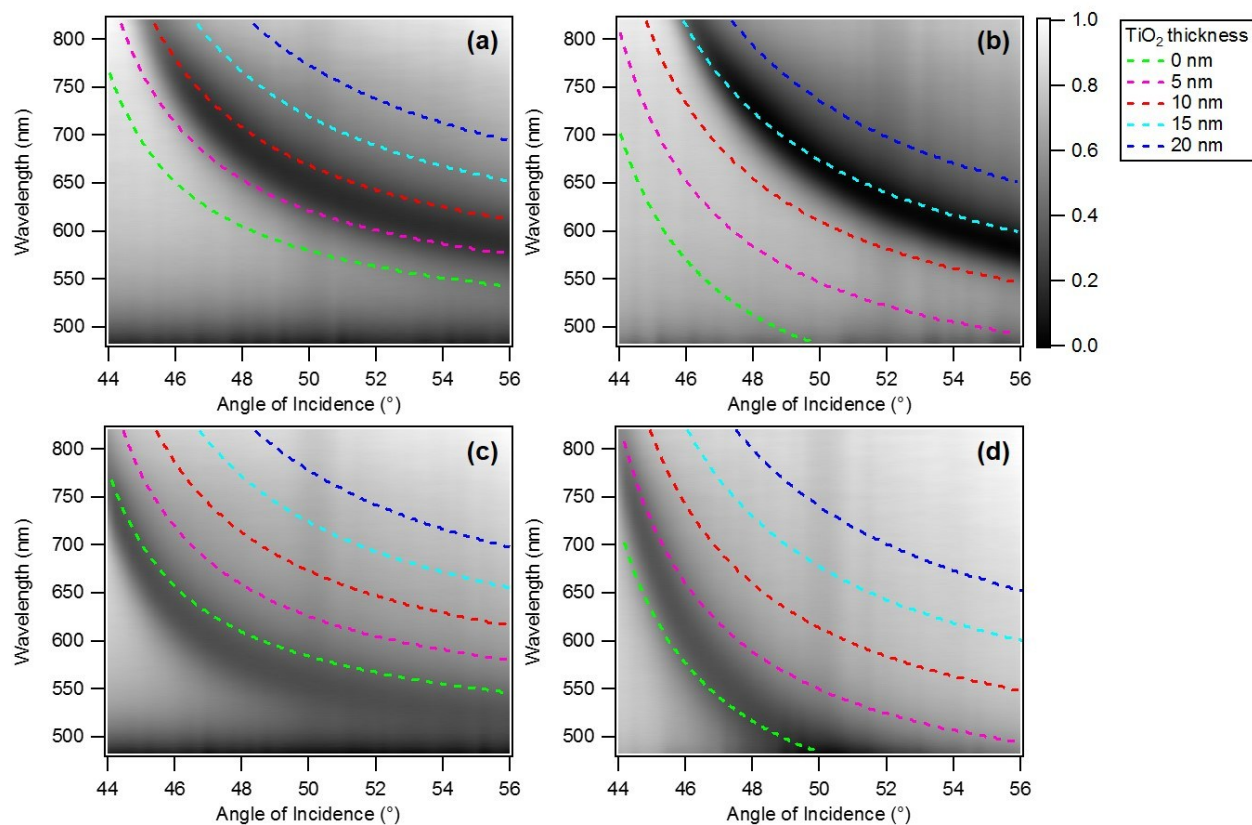


**Figure S1.** SPP dispersion curves. Measured SPP dispersion curves (black and white contour) for (a) Cr/Au/TiO<sub>2</sub> (2/40/10±5 nm), (b) Cr/Ag/TiO<sub>2</sub> (2/40/10±5 nm), (c) Cr/Au (2/40 nm), and (d) Cr/Ag (2/40 nm) are overlaid with simulated dispersion curves (color dashed lines) with varying TiO<sub>2</sub> thicknesses.

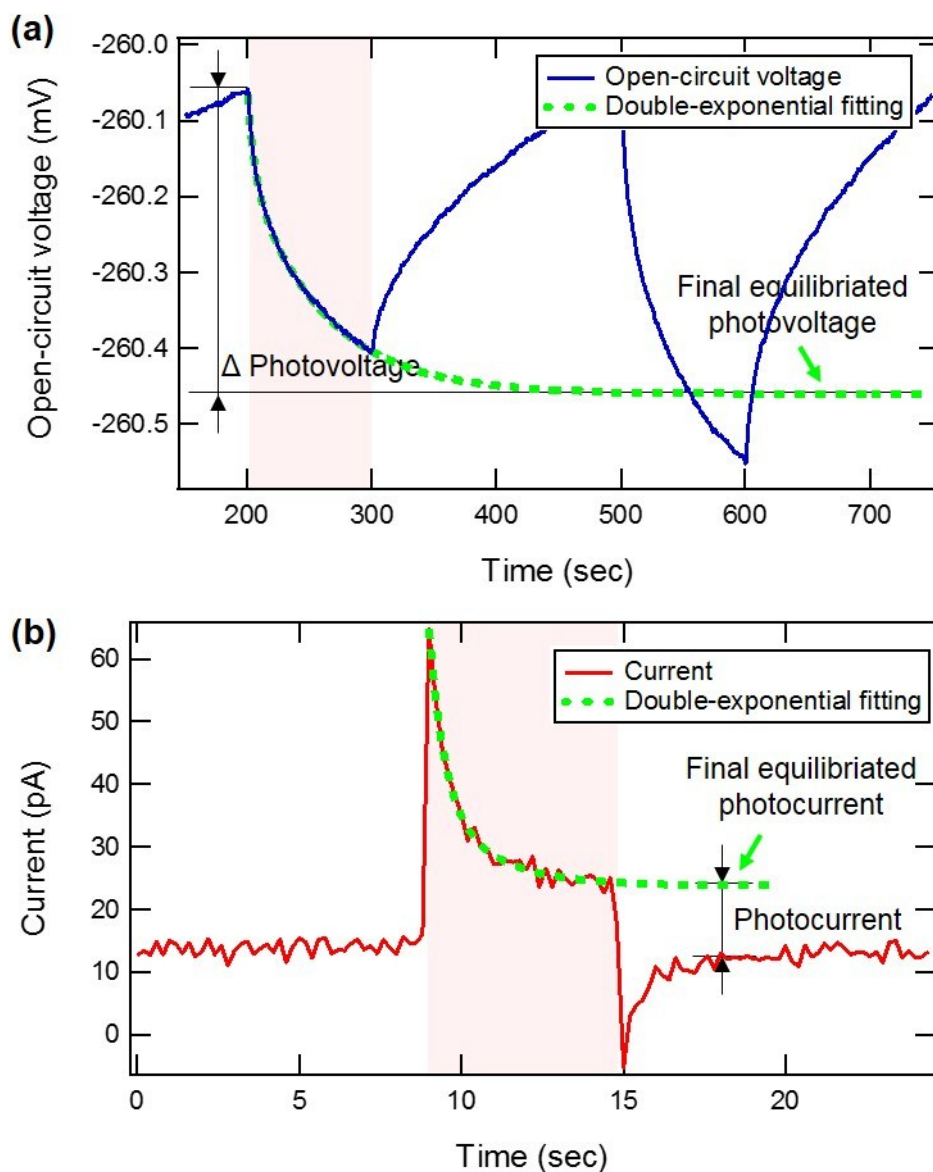


**Figure S2.** Data processing for photovoltage and photocurrent responses. A double-exponential function was fitted to the light irradiated regions (red shades) of (a) open-circuit voltage and (b) current curves to obtain the final equilibrated values (green dash lines) and  $\Delta$  values (black arrows).

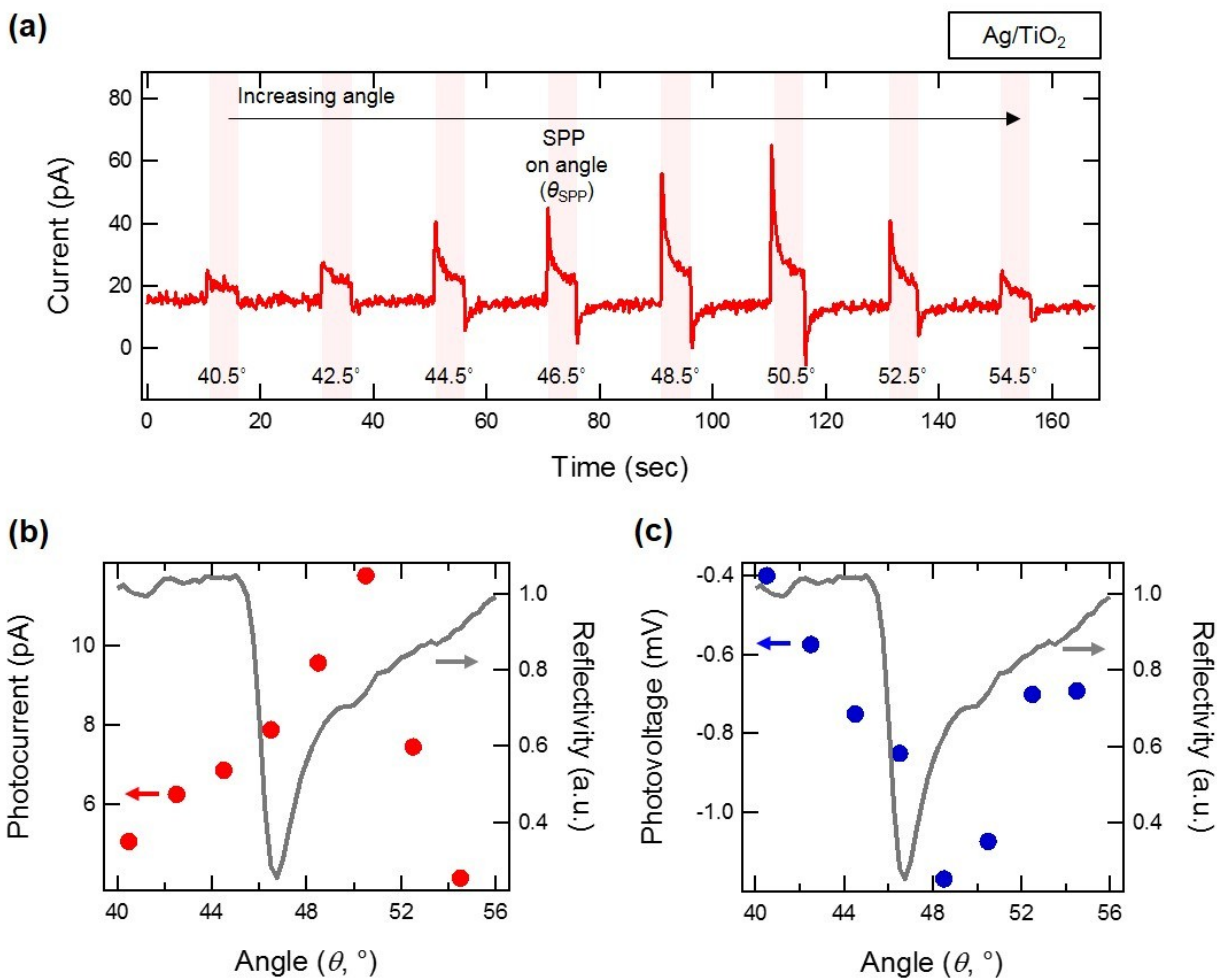


**Figure S3.** Anodic half-reaction of photocatalytic water-splitting. A Ag/TiO<sub>2</sub> deposited half-ball lens was in contact with methanol-free sodium hydroxide solution (0.1 M) and illuminated with 785 nm laser (red shaded regions). (a) Dependence of current on the incident angle of light. Angle dependent photocurrent (b) and photovoltage (c) plotted with a SPP resonance spectrum at 785 nm (gray line). A small positive bias of 0.20 V was applied during the current measurement.

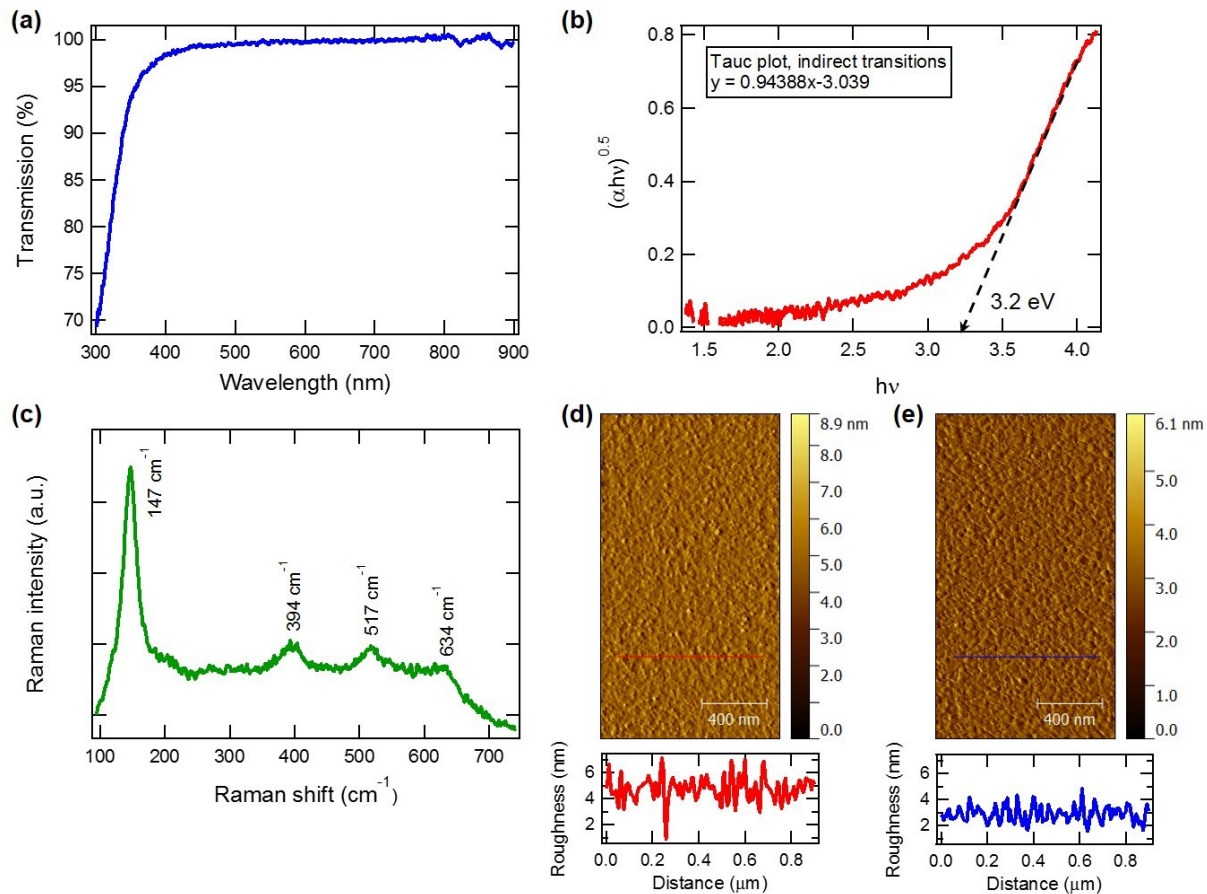


**Figure S4.** Characterization of ALD grown  $\text{TiO}_2$  films. (a) % transmission of a 10 nm thick  $\text{TiO}_2$  layer approaches  $\sim 100\%$  above  $\lambda = \sim 390$  nm, from which a band gap ( $E$ ) of the  $\text{TiO}_2$  film can be calculated as 3.2 eV using an equation,  $E = hc/\lambda$ , where  $h$  is Planck's constant and  $c$  is speed of light. The calculated band gap agrees well with results from the Tauc plot (b) that extrapolates a band gap of the ALD grown  $\text{TiO}_2$  to 3.2 eV, which is a band gap of anatase  $\text{TiO}_2$ . (c) Raman spectrum of a  $\text{TiO}_2$  layer ( $\sim 70$  nm thickness, on top of Cr/Au, 2/40 nm thickness) also indicates that the  $\text{TiO}_2$  films that we grow by ALD have an anatase crystalline structure, showing anatase characteristic Raman peaks.<sup>5</sup> It is known that peaks at 147 and 634  $\text{cm}^{-1}$  are by symmetric stretching vibration of O-Ti-O, a peak at 394  $\text{cm}^{-1}$  is by symmetric bending vibration of O-Ti-O, and a peak at 517  $\text{cm}^{-1}$  is by antisymmetric bending vibration of O-Ti-O.<sup>6</sup> Atomic force microscope images and cross-section profiles show that ALD grown  $\text{TiO}_2$  on top of Cr/Au films (d) has  $\sim 2$  nm increased roughness than  $\text{TiO}_2$ -free Cr/Au (e).



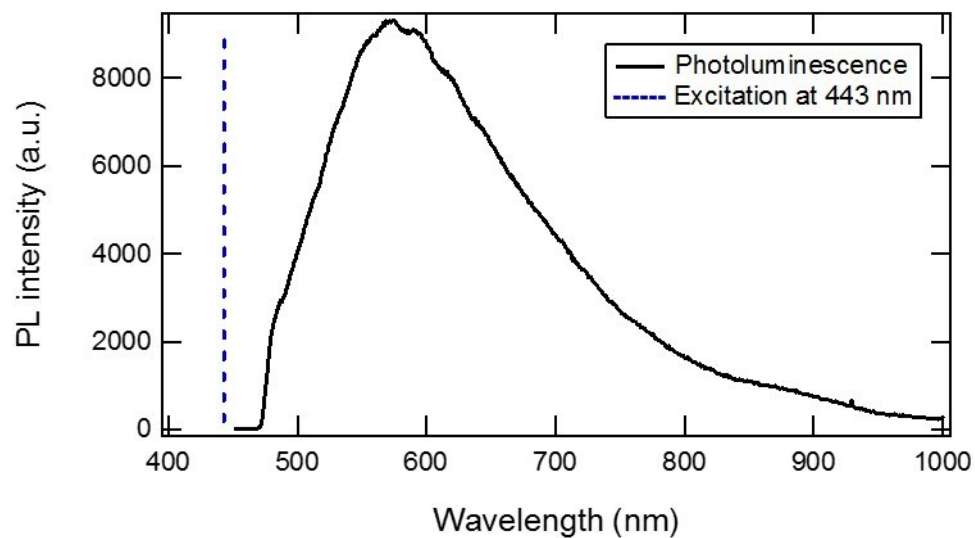


**Figure S5.** Photoluminescence from a TiO<sub>2</sub> layer. PL intensity was acquired from ~70 nm thick TiO<sub>2</sub> film grown by ALD on top of Cr/Au (2/40 nm thickness) on a glass substrate. A 443 nm laser (blue dash line) was used as an excitation source with 460 dichroic and 480 nm long pass filters.

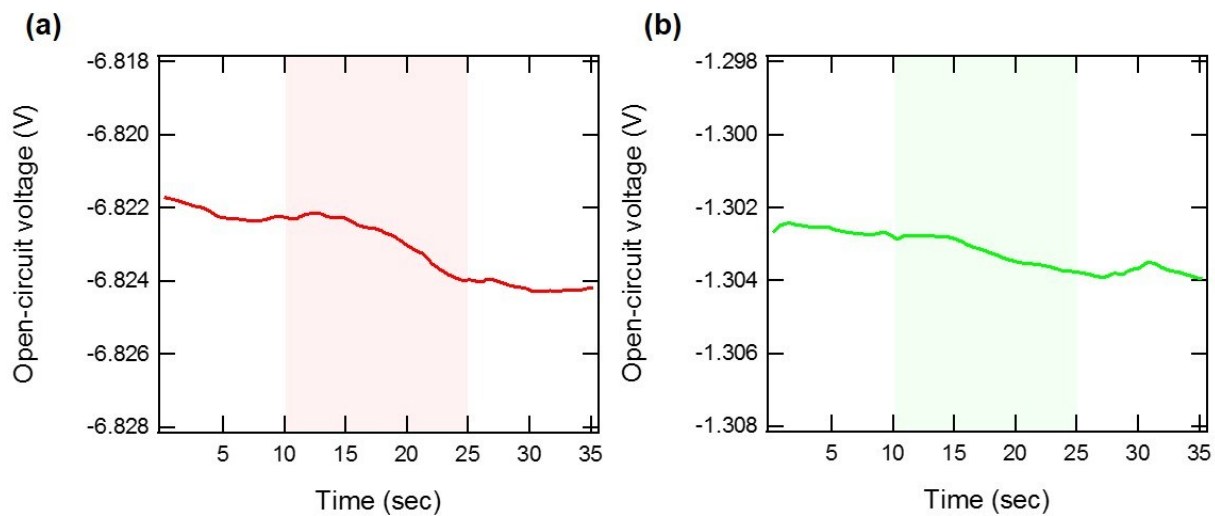


**Figure S6.** Open-circuit voltage of a bare TiO<sub>2</sub> film. A TiO<sub>2</sub> film in the absence of the metal film showed no light-induced photovoltage responses upon (a) 785 and (b) 532 nm laser irradiation (red and green shaded regions, respectively).

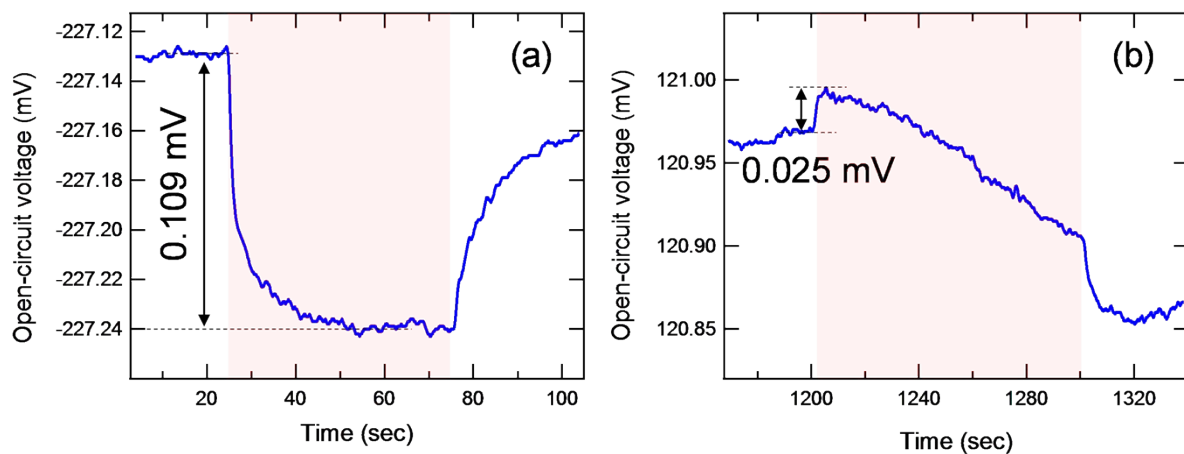


**Figure S7.** Open-circuit voltage versus time profiles of (a) Au/TiO<sub>2</sub> and (b) Au only system. A 785 nm laser (red shades) was incident on each system at their SPP resonant angles.

## References

- (1) Dahotre, N. B.; Harimkar, S. P. *Laser Fabrication and Machining of Materials*, Springer Science and Business Media, New York, NY, 2008; pp 40 - 42.
- (2) Takata, Y.; Haneda, H.; Mitsuhashi, T.; Wada, Y. Evaluation of Thermal Diffusivity for Thin Gold Films Using Femtosecond Laser Excitation Technique, *Appl. Surf. Sci.*, **2002**, *189*, 227-233.
- (3) Sze, S. M. *Physics of Semiconductor Devices*, 1<sup>st</sup> Ed; Wiley-Interscience: Murray Hill, NJ, 1969; p 111.
- (4) Enright, B.; Fitzmaurice, Spectroscopic Determination of Electron and Hole Effective Masses in a Nanocrystalline Semiconductor Film. *J. Phys. Chem.* **1996**, *100*, 1027-1035.
- (5) Ohsaka, T.; Izumi, F.; Fujiki, Y. Raman Spectrum of Anatase, TiO<sub>2</sub>. *Journal of Raman Spectroscopy* **1978**, *7*, 321-324.
- (6) Tian, F.; Zhang, Y.; Zhang, J.; Pan, C. Raman Spectroscopy: A New Approach to Measure the Percentage of Anatase TiO<sub>2</sub> Exposed (001) Facets. *J. Phys. Chem. C.* **2012**, *116*, 7515-7519.